AMERICAN SOCIETY FOR MICROBIOLOGY | Journal of Bacteriology

A *Sinorhizobium meliloti* RpoH-Regulated Gene Is Involved in Iron-Sulfur Protein Metabolism and Effective Plant Symbiosis under Intrinsic Iron Limitation

Shohei Sasaki, Kiwamu Minamisawa, Hisayuki Mitsui

Graduate School of Life Sciences, Tohoku University, Katahira, Aoba-ku, Sendai, Japan

ABSTRACT

In *Sinorhizobium meliloti*, RpoH-type sigma factors have a global impact on gene expression during heat shock and play an essential role in symbiosis with leguminous plants. Using mutational analysis of a set of genes showing highly RpoH-dependent expression during heat shock, we identified a gene indispensable for effective symbiosis. This gene, designated *sufT*, was located downstream of the *sufBCDS* homologs that specify the iron-sulfur (Fe/S) cluster assembly pathway. The identified transcription start site was preceded by an RpoH-dependent promoter consensus sequence. SufT was related to a conserved protein family of unknown molecular function, of which some members are involved in Fe/S cluster metabolism in diverse organisms. A *sufT* mutation decreased bacterial growth in both rich and minimal media, tolerance to stresses such as iron starvation, and activities of some Fe/S cluster-dependent enzymes. These results support the involvement of SufT in SUF (sulfur mobilization) system-mediated Fe/S protein metabolism. Furthermore, we isolated spontaneous pseudorevertants of the *sufT* mutant with partially recovered growth; each of them had a mutation in *rirA*. This gene encodes a global iron regulator whose loss increases the intracellular iron content. Deletion of *rirA* in the original *sufT* mutant improved growth and restored Fe/S enzyme activities and effective symbiosis. These results suggest that enhanced iron availability compensates for the lack of SufT in the maintenance of Fe/S proteins.

IMPORTANCE

Although RpoH-type sigma factors of the RNA polymerase are present in diverse proteobacteria, their role as global regulators of protein homeostasis has been studied mainly in the enteric gammaproteobacterium *Escherichia coli*. In the soil alphaproteobacterium *Sinorhizobium meliloti*, the *rpoH* mutations have a strong impact on symbiosis with leguminous plants. We found that *sufT* is a unique member of the *S. meliloti* RpoH regulon; *sufT* contributes to Fe/S protein metabolism and effective symbiosis under intrinsic iron limitation exerted by RirA, a global iron regulator. Our study provides insights into the RpoH regulon function in diverse proteobacteria adapted to particular ecological niches and into the mechanism of conserved Fe/S protein biogenesis.

Bacteria of the phylum *Proteobacteria* have very diverse shape, metabolic capacity, and ecological significance and are adapted to diverse environments. The alphaproteobacterium *Sinorhizobium meliloti* inhabits the soil and engages in nitrogen-fixing symbiosis with its compatible legume hosts (genera *Medicago*, *Melilotus*, and *Trigonella*), in which bacterially fixed nitrogen is exchanged for host photosynthates and enables the host to grow without a nitrogen supply. *S. meliloti* elicits the formation of nodules from the root cortex and invades the developing nodule cells through a host-derived structure termed an "infection thread." The internalized bacteria terminally differentiate to become nitrogen-fixing bacteroids; their differentiation is driven by a family of host-derived antimicrobial peptides called NCR peptides (1, 2).

Bacterial transcription is directed by the multisubunit RNA polymerase, in which the sigma factor confers promoter recognition and transcription initiation on the core enzyme with a subunit composition of $\alpha_2\beta\beta'\omega$ (3). In bacteria, a single housekeeping sigma factor recognizes the majority of promoters, and an additional "alternative sigma factor(s)," which replaces the housekeeping one, redirects RNA polymerase to a specialized set of genes in response to physiological or environmental cues. Among these sigma factors, σ^{32} (RpoH) initiates transcription of genes encoding molecular chaperones and proteases in the gammaproteobacterium *Escherichia coli* (3, 4). The intracellular level and activity of σ^{32} increase in response to a temperature increase or other stresses that destabilize and denature proteins, so that the upregulated regulon members, termed heat shock proteins (Hsps), refold stress-denatured proteins, prevent protein aggregation, or target terminally misfolded proteins for proteolytic degradation (5); together, these processes are referred to as the heat shock response. RpoH homologs are widespread within the *Proteobacteria*, and the view that RpoH is a global regulator for re-

Received 7 April 2016 **Accepted** 9 June 2016

Accepted manuscript posted online 13 June 2016

Citation Sasaki S, Minamisawa K, Mitsui H. 2016. A *Sinorhizobium meliloti* RpoH-regulated gene is involved in iron-sulfur protein metabolism and effective plant symbiosis under intrinsic iron limitation. J Bacteriol 198:2297–2306. doi:10.1128/JB.00287-16.

Editor: A. Becker, Philipps-Universität Marburg

Address correspondence to Hisayuki Mitsui, hmitsui@ige.tohoku.ac.jp.

Supplemental material for this article may be found at http://dx.doi.org/10.1128/JB.00287-16.

sponding to heat shock and other stresses has prevailed among researchers studying various proteobacteria (6–12).

The *S. meliloti* genome encodes the housekeeping sigma factor SigA (also called RpoD) and 14 alternative sigma factors, including RpoN, RpoH1, RpoH2, and extracytoplasmic function sigmas (RpoE1 to RpoE10 and FecI) (8, 13, 14). The presence of multiple RpoHs is common to many alphaproteobacteria, including other legume-symbiotic bacteria (11, 12, 15). In *S. meliloti*, an *rpoH1* mutation reduces the expression of more than 300 genes during heat shock or acidic pH stress; these genes include homologs of the *E. coli* σ^{32} regulon members that encode major chaperones or proteases such as ClpB, DnaK, GroEL, and Lon (16–19). An *rpoH2* mutation affects the expression of at least 44 genes during late stationary-phase growth, but none during heat shock (19). In addition, the *rpoH* mutations cause notable symbiotic defects in *S. meliloti*; the *rpoH1* mutant elicits nodules with no nitrogen-fixing activity (Fix$^-$ phenotype) (8, 13, 16). The *rpoH2* mutant shows no notable phenotypic changes, whereas symbiotic defects are more severe in the *rpoH1 rpoH2* double mutant than in the *rpoH1* single mutant and include the lack of nodule formation (Nod$^-$ phenotype); this indicates a partially redundant role of RpoH2 in symbiosis (8, 13, 16, 17). Thus, it appears that the cellular role of RpoHs has been diversified in the distinct lifestyles of bacteria; however, none of the known regulon members explain the symbiotic role of RpoH in *S. meliloti*.

In almost all organisms, metalloproteins containing iron-sulfur (Fe/S) clusters (inorganic cofactors consisting of ferrous or ferric iron and sulfidic sulfur) participate in diverse cellular processes such as respiration, metabolism, DNA replication and repair, and regulation of gene expression (20, 21). The well-conserved systems responsible for Fe/S protein biogenesis in both prokaryotes and eukaryotes are the SUF (sulfur mobilization) system and the ISC (iron-sulfur cluster) system (22–25). In the former, the SufS-SufE complex serves as a sulfur donor, and the SufB-SufC-SufD complex acts as a scaffold that allows iron and sulfur to form a cluster; the iron donor remains unclear. These proteins thus serve for *de novo* assembly of Fe/S clusters. SufA is an A-type carrier suggested to have a [4Fe-4S] cluster-specific function (26, 27). In *S. meliloti*, homologs of those SUF components are encoded by the gene cluster *sufBCDS*-SMc00302-*sufA* (Fig. 1A) and the separate gene *sufE* (SMc00118) (14); interestingly, expression of SMc00302 and *sufA* increases in an RpoH-dependent manner during heat shock or acidic pH stress (18, 19). Apparently, *S. meliloti* does not have the ISC system. Here, we conducted mutational analysis of the RpoH regulon in *S. meliloti* and identified SMc00302 as a gene that is necessary for effective symbiosis; it is likely involved in metabolism of Fe/S proteins. This work reinforces a central role of the RpoH regulon in the maintenance of protein homeostasis.

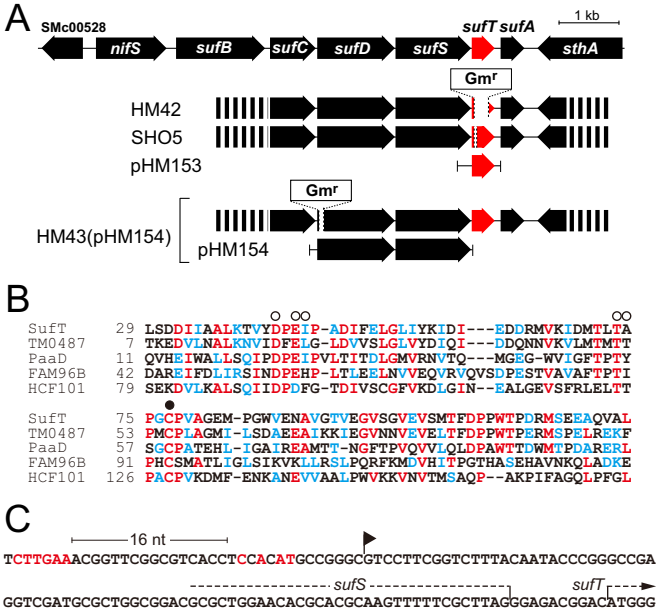

FIG 1 *Sinorhizobium meliloti* SMc00302/*sufT*. (A) Schematic representation of the chromosomal *suf* region (RefSeq accession number NC_003047) and the regions deleted from the chromosome or cloned into the plasmids in this study. Gm^r, a gentamicin-resistance gene cassette inserted into the chromosome. (B) Multiple alignment of amino acid sequences of *S. meliloti* SufT (126 amino acids in total; CAC46310) and other DUF59 family members: *Thermotoga maritima* TM0487 (103 amino acids; 1WCJ_A), *E. coli* PaaD (165 amino acids; P76080), human FAM96B (163 amino acids; Q9Y3D0), and *Arabidopsis thaliana* HCF101 (532 amino acids; Q6STH5). Red, identical amino acids; blue, amino acids with similar properties. Circles above the alignment indicate residues that form the putative active site in TM0487 (67). A closed circle indicates a hyperreactive cysteine residue predicted in FAM96B (68). (C) Nucleotide sequence upstream of *sufT*. The 3′-terminal and 5′-terminal regions of the *sufS* and *sufT* ORFs, respectively, are shown with dashed lines. A flag sign indicates the terminus of the longest *sufT* cDNA obtained by 5′ RACE. Nucleotides matching the consensus for the RpoH1-dependent promoter (CTTGAA-N$_{15–16}$-CCTATAT) (19) are shown in red.

and chloramphenicol (Cm) were used at the concentrations previously described (8). Clones of *S. meliloti* harboring *sacB* were counterselected on solid LB-MC medium containing 5% sucrose. For nodulation assays, seeds of alfalfa (*Medicago sativa*) were surface sterilized in 1% sodium hypochlorite solution for 15 min, rinsed in sterilized water, and germinated on a 1% agar plate for 2 days. The seedlings were transferred onto vermiculite soaked with Jensen's nitrogen-free medium (30) in an assembly of two 300-ml plastic containers (following the Leonard jar) (30). *S. meliloti* cells that were grown to an optical density at 660 nm (OD$_{660}$) of 0.3 to 1.0 in liquid LB-MC medium were collected, washed with 0.85% saline, and resuspended in sterilized water to an OD$_{660}$ of ~0.02. The suspension (5 ml) was added to a jar assembly containing five seedlings, which was then placed in a growth chamber held at 25°C with a photoperiod regime of 16 h of illumination and 8 h of darkness.

Genetic techniques. Plasmids were transferred by conjugation from *E. coli* DH5α into *S. meliloti* strains by triparental mating with the mobilizing strain MT616 (31). General transduction of *S. meliloti* was conducted using phage ϕM12 (29).

Strain and plasmid construction. Bacterial strains and plasmids used in this work are listed in Table 1 (see also Tables S2 to S4 in the supplemental material). PCR primers are listed in Table S1 in the supplemental material. The following plasmids were generated from pFAJ1702 by cloning PCR-amplified fragments: pHM153 carried a 725-bp region covering the *sufT* open reading frame (ORF) and the associated RpoH promoter

MATERIALS AND METHODS

Bacterial growth conditions and plant nodulation assay. *Escherichia coli* strains were grown at 37°C in rich medium (Luria-Bertani [LB] medium) (28); *S. meliloti* strains were grown at 25°C in LB medium, LB medium supplemented with $MgCl_2$ (2.5 mM) and $CaCl_2$ (2.5 mM) (LB-MC medium) (29), or minimal medium (M9 medium) (28) supplemented with a carbon source (e.g., sucrose) to 0.1% for liquid medium or 0.2% for solid medium (unless indicated otherwise), biotin (1 μg ml^{-1}), and $CoCl_2$ (10 ng ml^{-1}) (called M9-sucrose, etc., here). Agar was added to 1.5% for the solid media. The antibiotics streptomycin (Sm), gentamicin (Gm), neomycin (Nm), kanamycin (Km), spectinomycin (Sp), tetracycline (Tc),

TABLE 1 Strains and plasmids used in this study

Strain or plasmid	Characteristic(s)	Reference or source
S. meliloti strains		
Rm1021	Wild type; Sm^r	69
BY294	Rm1021 *rpoH2*::*aacC1* Sm^r Gm^r	8
HY658N	Rm1021 *rpoH1*::*aphII* Sm^r Nm^r	8
HY658G	Rm1021 *rpoH1*::*aacC1* Sm^r Gm^r	8
HM9	Rm1021 *rpoH1*::*aphII rpoH2*::*aacC1* Sm^r Nm^r Gm^r	8
HM13	Rm1021 Δ*clpB*::*aacC1* Sm^r Gm^r	This work
HM20	Rm1021 Δ(*hslV*-SMc02576-*hslU*)::*aacC1* Sm^r Gm^r	This work
HM21	Rm1021 ΔSMc03794::*aacC1* Sm^r Gm^r	This work
HM22	Rm1021 Δ(SMb21296-SMb21295-SMb21294)::*aacC1* Sm^r Gm^r	This work
HM25	Rm1021 SMc00949::*aacC1* Sm^r Gm^r	This work
HM26	Rm1021 *ibpA*::*aacC1* Sm^r Gm^r	This work
HM27	Rm1021 ΔSMb21296::*aacC1* Sm^r Gm^r	This work
HM28	Rm1021 SMc02769::*aacC1* Sm^r Gm^r	This work
HM41	Rm1021 *ibpA*::*aphII* SMb21295::*aadA* Δ(SMc01106-SMc01107)::*aacC1* Sm^r Gm^r Nm^r Sp^r	This work
HM42	Rm1021 Δ*sufT*::*aacC1* Sm^r Gm^r	This work
HM43(pHM154)	Rm1021 Δ*sufD*::*aacC1*; carries pHM154; Sm^r Gm^r Tc^r	This work
HM45	Rm1021 SMc02886::*aacC1* Sm^r Gm^r	This work
HM46	Rm1021 *msrA1*::*aacC1* Sm^r Gm^r	This work
HM47	Rm1021 Δ(SMc02882-SMc02883)::*aacC1* Sm^r Gm^r	This work
HM48	Rm1021 Δ(SMb21257-SMb21258-SMb21259)::*aacC1* Sm^r Gm^r	This work
HM49	Rm1021 Δ*htpG*::*aacC1* Sm^r Gm^r	This work
HM51	Rm1021 *rpoH1*::*aphII* Δ*rirA*::*aacC1* Sm^r Nm^r Gm^r	This work
HM1127	Rm1021 with single crossover of pHM127 in *gst7*; Sm^r Nm^r	This work
HM1128	Rm1021 with single crossover of pHM128 in SMc03152; Sm^r Nm^r	This work
HM1129	Rm1021 with single crossover of pHM129 in SMc04202; Sm^r Nm^r	This work
HM1130	Rm1021 with single crossover of pHM130 in SMb20551; Sm^r Nm^r	This work
HM1134	Rm1021 with single crossover of pHM134 in *htpX*; Sm^r Nm^r	This work
HM1135	Rm1021 with single crossover of pHM135 in SMc03968; Sm^r Nm^r	This work
HM1136	Rm1021 with single crossover of pHM136 in SMc03246; Sm^r Nm^r	This work
HM1137	Rm1021 with single crossover of pHM137 in SMc03837; Sm^r Nm^r	This work
HM1143	Rm1021 with single crossover of pHM143 in SMc03802; Sm^r Nm^r	This work
HM1152	Rm1021 with single crossover of pHM152 in SMc03801; Sm^r Nm^r	This work
HM1158	Rm1021 with single crossover of pHM158 in SMc01759; Sm^r Nm^r	This work
HM1159	Rm1021 with single crossover of pHM159 in *sufA*; Sm^r Nm^r	This work
HM1160	Rm1021 with single crossover of pHM160 in SMc00341; Sm^r Nm^r	This work
HM1161	Rm1021 with single crossover of pHM161 in *sohB*; Sm^r Nm^r	This work
HM1164	Rm1021 with single crossover of pHM164 in SMa0291; Sm^r Nm^r	This work
SHO101	Rm1021 with single crossover of pSHO1 in *creA*; Sm^r Nm^r	This work
SHO102	Rm1021 with single crossover of pSHO2 in SMc00591; Sm^r Nm^r	This work
SHO5	Rm1021 Δ*sufT*; Sm^r	This work
SHO8	Spontaneous pseudorevertant of SHO5 regarding slow growth; Sm^r	This work
SHO9	Spontaneous pseudorevertant of SHO5 regarding slow growth; Sm^r	This work
SHO16	Spontaneous pseudorevertant of SHO5 regarding slow growth; Sm^r	This work
SHO23	Rm1021 Δ*rirA*::*aacC1* Sm^r Gm^r	This work
SHO24	Rm1021 Δ*sufT* Δ*rirA*::*aacC1* Sm^r Gm^r	This work
E. coli strains		
DH5α	F^- ϕ80d*lacZ*ΔM15 Δ(*lacZYA-argF*)*U169 hsdR17*(r_K^- m_K^+) *recA1 endA1 relA1 deoR supE44 thi-1 gyrA96* λ^-	Nippon Gene
MT616	Conjugation helper strain carrying pRK600; Cm^r	31
Plasmids[a]		
pRK600	Cm^r; ColE1 replicon with RK2 *tra* genes	31
pMS246	*aacC1* (Gm^r) gene cassette	70
pHP45Ω	*aadA* (Sm^r-Sp^r) gene cassette	71
pUC4KIXX	*aphII* (Km^r-Nm^r) gene cassette	Pharmacia
pK18mob/pK19mob	Km^r-Nm^r; mobilizable vector with pMB1 replicon, does not replicate in *S. meliloti*	72
pK18mobsacB	Km^r-Nm^r; pK18mob derivative with *sacB*	72
pGMS2	Gm^r; pK18mobsacB derivative with replacement of Km^r by Gm^r	73

(Continued on following page)

TABLE 1 (Continued)

Strain or plasmid	Characteristic(s)	Reference or source
pFAJ1702	Tc^r; IncP broad-host-range vector	74
pHC41	Tc^r; IncP broad-host-range vector	75
pAS1	Tc^r; pFAJ1702 derivative with the *groES1* promoter	This work
pHM102	Tc^r; pAS1 derivative with *groES1p-rpoH1*	This work
pHM153	Tc^r; pFAJ1702 derivative with *sufT*$^+$	This work
pHM154	Tc^r; pHC41 derivative with *sufDS*$^+$	This work
pSHO6	Tc^r; pAS1 derivative with *groES1p-sufT*$^+$	This work
pHM186	Tc^r; pFAJ1702 derivative with *rirA*$^+$	This work

[a] Plasmids used for gene disruption in Rm1021 are listed in Tables S2 to S4 in the supplemental material.

consensus sequence; pHM186, a 685-bp region covering the *rirA* ORF; and pAS1, a 253-bp region containing *groES1p*. Two plasmids were generated from pAS1 by cloning PCR-amplified fragments: pHM102 contained a 932-bp region covering the *rpoH1* ORF and pSHO6 contained a 553-bp region covering the *sufT* ORF (neither of the two regions contained a promoter). pHM154 was generated by PCR amplification of a 2,689-bp region covering the *sufDS* ORFs and cloning it into pHC41.

Some RpoH-dependent genes were disrupted using plasmids generated by PCR amplification of internal portions of their ORFs and cloning the PCR fragments into pK18mob or pK19mob (see Table S2 in the supplemental material). Each of the resulting plasmids was transferred by conjugation into Rm1021, and the cells were selected for Sm^r and Nm^r to obtain a single-crossover insertion of the plasmid into the genomic region corresponding to the cloned region.

Gm^r, Nm^r, or Sm^r-Sp^r gene cassette insertions or corresponding resistance-marked deletions in some RpoH-dependent genes were generated by cloning a restriction fragment from total *S. meliloti* DNA into pK18mob, pK19mob, or pGMS2 and then inserting the cassette into a restriction site(s) within the ORF of the target gene (see Table S3 in the supplemental material). Gm^r cassette insertions or corresponding resistance-marked deletions in other RpoH-dependent genes, *rirA*, and *sufD* were generated by PCR amplification of a pair of flanking regions of the gene, cloning the two regions together into pK18mob, pK19mob, or pK18mobsacB, and then inserting the Gm^r cassette into a synthetic restriction site between the cloned two regions (see Table S4 in the supplemental material). The Gm^r cassette was excised from pMS246, the Nm^r cassette from pUC4KIXX, and the Sm^r-Sp^r cassette from pHP45Ω. Except for the case of *sufD* disruption, each resulting plasmid was transferred by conjugation into Rm1021 (or BY294 when the Sm^r-Sp^r cassette was used), and cells were selected for Sm^r (or Gm^r when BY294 was used as a recipient), resistance conferred by the inserted cassette, and Nm sensitivity (or sucrose resistance when pK18mobsacB or pGMS2 was used) to obtain double crossover between the plasmid and the genomic region corresponding to the cloned region. Then, Rm1021 was transduced with a ϕM12 lysate of the resistant clone. One of the resulting strains, SHO23, was further transduced with a lysate prepared from the *rpoH1* mutant (HY658N) to yield HM51 (Nm^r). For *sufD*, the plasmid generated (derived from pK18mobsacB) was transferred by conjugation into Rm1021, and an Sm^r Gm^r Nm^r transconjugant was selected for single-crossover insertion of the plasmid into the flanking region of *sufD* on the chromosome. Next, pHM154 was also transferred by conjugation into the selected clone, and a transconjugant showing sucrose resistance and Sm^r, Gm^r, Tc^r, and Nm sensitivity was selected for double-crossover insertion of the Gm^r cassette into *sufD* on the chromosome in the presence of pHM154.

A marker-free deletion in *sufT* was generated by PCR amplification of the upstream and downstream flanking regions and cloning the two fragments into pK18mobsacB; the inserts replaced 72 nucleotides (nt) of the ORF with GATC (see Table S4 in the supplemental material). The resulting plasmid was transferred by conjugation into HM42 (Δ*sufT*::Gm^r). An Sm^r Nm^r transconjugant was selected for single-crossover insertion of the plasmid into a flanking region of *sufT* on the chromosome, grown in LB-MC medium lacking Nm, and rescreened for sucrose-resistant colonies. The clones selected were further screened for Nm and Gm sensitivity, yielding SHO5. SHO24 was obtained by transducing SHO5 with an SHO23 lysate (Gm^r).

All generated strains were checked by PCR using the primers listed in Table S1 in the supplemental material to confirm the proper marker insertions or deletions.

Doubling time measurements and hydrogen peroxide sensitivity assays. A single colony was transferred from solid LB-MC or M9-sucrose medium into the corresponding liquid medium. The culture was grown to an OD_{660} of 0.3 to 0.4 and then diluted to an OD_{660} of 0.01 with the same medium with no antibiotics. The growth was followed by monitoring the OD_{660} every 30 min for LB-MC cultures or every 1 h for M9-sucrose cultures. The doubling time was calculated from the OD_{660} values, ranging from 0.05 to 0.16.

To test for hydrogen peroxide (H_2O_2) sensitivity, an LB-MC culture grown to an OD_{660} of 0.1 was diluted 1:200 with M9-sucrose medium, resulting in a density of $\approx 4 \times 10^5$ CFU ml^{-1}. Then H_2O_2 was added to an indicated concentration, and the culture was incubated at 25°C with shaking. We determined the CFU of the culture immediately before and 30 min after H_2O_2 addition by plating it on solid LB-MC medium and incubating the plates for 5 days at 25°C.

Enzyme assays. *Sinorhizobium meliloti* cells were grown in liquid M9-sucrose medium (containing 0.2% sucrose) to an OD_{660} of 0.3, chilled on ice, and collected by centrifugation. Cell pellets were resuspended in a 1.3% volume of cold 50 mM Tris-HCl (pH 7.65) supplemented with complete EDTA-free protease inhibitor cocktail (Roche Applied Science) under nitrogen gas and lysed by sonication in a sealed tube using acoustic solubilizer (Covaris). The lysate was centrifuged at 17,000 × *g* for 5 min, and the supernatant was frozen in liquid nitrogen and stored at −80°C until use. Total protein was quantified using the protein assay dye reagent (Bio-Rad) with bovine γ-globulin as a standard. The activity of 6-phosphogluconate dehydratase (6-PGDH) was examined with 6-phosphogluconate (6-PG) as a substrate as follows: (i) 6-PGDH converts 6-PG into 2-keto-3-deoxygluconate 6-phosphate (KDGP), and then KDGP aldolase (both enzymes are present in the cell lysate) converts KDGP into pyruvate and glyceraldehyde 3-phosphate; and (ii) the amount of pyruvate is quantified using lactic dehydrogenase and NADH (32). In parallel, the assay was performed with KDGP as a substrate to verify that the rate-limiting enzyme for pyruvate production was 6-PGDH. Aconitase activity measurements were based on the formation of *cis*-aconitate from isocitrate (33). Glutamate synthase (GltS) activity was measured by the rate of NADPH oxidation in the presence of 2-oxoglutarate and L-glutamine (34). Malate dehydrogenase activity was measured by the rate of NADH oxidation in the presence of oxaloacetate (35). To ensure the detection of oxygen-labile activity, we used a glove box into which nitrogen gas flowed from a high-pressure gas cylinder for all the enzyme assays at room temperature (≈22°C), except that pyruvate was quantified under ambient air. 6-PG, isocitrate, 2-oxoglutaric acid, L-glutamine, and oxalacetic acid were purchased from Wako Pure Chemical Industries. NADH, NADPH, lactic dehydrogenase (bovine heart), and KDGP were purchased from Sigma-Aldrich.

Whole-genome resequencing. Total DNA was processed using the Nextera DNA sample preparation kit (Illumina) to generate a shotgun library with unique index adapters. The libraries from strains Rm1021, SHO5, SHO8, SHO9, and SHO16 were sequenced on a MiSeq system (Illumina), yielding the following numbers of 250-bp paired-end reads: 2.7×10^6, 2.3×10^6, 2.5×10^6, 2.3×10^6, and 2.5×10^6, respectively. We used a 21-nt window to scan the reads for sequence variants versus the reference *S. meliloti* Rm1021 genome sequence in the GenBank database (RefSeq accession numbers NC_003037, NC_003047, and NC_003078) by using the "missing *k*-mer" tool of ShortReadManager (36). Using each of the retrieved sequences, we collected all of the reads containing a 20-nt sequence adjacent to the variation point by using ShortReadManager and aligned the sequences of those reads in Microsoft Excel. If all, or all but one, of at least 15 collected reads had the same variant, we concluded that the corresponding mutation was present in the strain. Mutations found only in SHO8, SHO9, or SHO16 were sorted from ones common between these three strains and Rm1021 or SHO5. The resulting mutations were derived from the variants found in all of the 18 to 62 reads that were collected above individually in SHO8, SHO9, and SHO16.

RESULTS

Symbiotic phenotypes of *S. meliloti* strains with mutations in RpoH-dependent heat shock-induced genes. On the basis of global transcription profiling of the wild type versus single or double *rpoH* mutants (growth, 30°C; heat shock, 42°C, 15 min), Barnett et al. reported a list of RpoH-regulon members in *S. meliloti* (19). We independently performed a transcriptome analysis with differences in the temperatures for growth (25°C) and heat shock (37°C, 10 min) and in analysis methods (see Materials and Methods in the supplemental material). From the list of Barnett et al. (19), we selected 35 presumed operons or solitary genes whose expression decreased most strongly in the *rpoH1 rpoH2* double mutant (strain HM9) compared to that in the wild type (strain Rm1021) in our analysis (see Table S5 in the supplemental material). Most of these transcription units also respond to heat shock in wild-type cells (19); in 26 of the transcription units, RpoH-dependent promoter consensus sequences precede the transcription start sites (16, 19, 37) (see Table S5). We disrupted 29 of the transcription units individually by using insertions of antibiotic resistance cassettes or resistance-marked deletions and confirmed operon disruption by PCR (see Table S5); mutants lacking *groEL4* and *groESL5* have been documented to be Fix$^+$ (16, 17). A triple mutant lacking the small Hsp homologs SMc04040 (*ibpA*), SMb21295, and SMc01106 (strain HM41) was also generated. In nodulation assays with alfalfa plants, all of the generated mutants except the one with a mutation in SMc00302 (see Table S5) supported healthy plant growth and formation of pink cylindrical nodules, indicating a Fix$^+$ phenotype. These included a strain with a mutation in *sufA*, the gene immediately downstream of SMc00302 (Fig. 1A). In contrast, mutants with deletions in SMc00302 (strain HM42, a Gm^r-marked deletion, and strain SHO5, a nonpolar marker-free deletion) (Fig. 1A) were unable to support normal plant growth, and small white nodules were formed, indicating a Fix$^-$ phenotype (see Fig. S1A in the supplemental material, plant in the middle). The Fix$^+$ phenotype was restored when HM42 (data not shown) or SHO5 (see Fig. S1A) was complemented with SMc00302 introduced in *trans* on the pHM153 plasmid (Fig. 1). Therefore, SMc00302 is indispensable for effective symbiosis.

SMc00302/SufT belongs to a conserved protein family related to Fe/S protein metabolism. The amino acid sequence of SMc00302 is similar to the sequences of the members of the DUF59 (domain of unknown function 59) family, which is widespread in prokaryotes and eukaryotes (Fig. 1B). Some of its members are involved in Fe/S protein metabolism. For example, PaaD serves for maturation of PaaE, a [2Fe-2S]-containing reductase component of phenylacetate-coenzyme A monooxygenase, in diverse bacteria (38). FAM96B, also known as MIP18 or CIA2B, is a component of the CIA (cytosolic iron-sulfur protein assembly) targeting complex, which interacts with target apoproteins and delivers Fe/S clusters to them in the cytosol of eukaryotic cells (39). In *Arabidopsis thaliana*, HCF101 serves for maturation of [4Fe-4S] cluster-containing proteins in the chloroplast (40). Genes encoding proteins of the DUF59 family are located in the *suf* operons of some bacteria such as *Mycobacterium tuberculosis* (41); such genes were recently named *sufT* (25). Thus, we postulated that the function of SMc00302 is related to the SUF system, and this gene is here referred to as *sufT*.

To clarify whether a *sufT* mutant would have the same phenotype as other *suf* mutants, we introduced a Gm^r-marked deletion into chromosomal *sufD* in the presence of plasmid-borne *sufDS* genes, yielding strain HM43(pHM154) (Fig. 1A). Then we examined the frequencies of transduction of Rm1021 and its pHM154-carrying derivative (i.e., a merodiploid for *sufDS*) for Gm^r using a ϕM12 lysate of HM43(pHM154). Rm1021(pHM154) gave rise to $1.5 \pm 0.3 \times 10^{-7}$ colonies per PFU (mean ± standard deviation; $n = 5$) at 25°C on Gm-containing LB medium; a Gm^r-marked deletion in *sufD* on the chromosome was confirmed by PCR in some of these colonies (data not shown). Under the same conditions, Rm1021 gave rise to $4.2 \pm 3.4 \times 10^{-9}$ colonies per PFU ($n = 5$) that grew slowly; we regarded them as false positives because they had a wild-type *sufD* allele but not the Gm^r cassette (data not shown). This indicates that *sufD* disruption is lethal (which one might expect from the absence of the ISC system) or, less likely, that it interrupts the transduction. Transduction of Rm1021 using an HM42 (Δ*sufT*::Gm^r) lysate produced $2.2 \pm 0.2 \times 10^{-7}$ Gm^r colonies per PFU ($n = 3$) under the same conditions. Taken together, these data suggest that SufT is distinct from the core SUF components and ancillary to the SUF system.

RpoH1-dependent transcription of *sufT*. Heat shock or mutations in *rpoH1* significantly affect the expression of *sufT* and *sufA* but not that of *sufBCDS* (19). Using quantitative reverse transcription-PCR, we verified that *sufT* expression was increased by heat shock in the wild type and the *rpoH2* mutant but not in the *rpoH1* mutant or *rpoH1 rpoH2* double mutant (see Fig. S1B in the supplemental material); 5′ rapid amplification of cDNA ends (RACE) also detected a *sufT* transcript that appeared during heat shock in the wild type but not in the *rpoH1 rpoH2* double mutant (see Fig. S1C in the supplemental material). Sequencing of the RACE product allowed us to map the transcription start site at nucleotide position 92 upstream of the *sufT* start codon, i.e., within the *sufS* ORF; transcription beginning at this position had been missed by the previous global studies. This site was preceded by an RpoH-dependent promoter consensus-like sequence (Fig. 1C). To examine whether ectopic expression of *sufT* alleviates the symbiotic defects of the *rpoH* mutant, we expressed *sufT* under the control of the RpoH-independent *groESL1* promoter (16). We introduced the pSHO6 plasmid carrying a *groESL1p-sufT* fusion into HY658N and SHO5 and assayed the strains obtained for plant nodulation. The Fix$^-$ phenotype of SHO5 but not that of HY658N was rescued by pSHO6, indicating that *sufT* was expressed from pSHO6 at a level sufficient for effective symbiosis. The Fix$^+$ phenotype was

TABLE 2 Impact of the *sufT* and *rirA* mutations on growth rates and enzyme activities of *Sinorhizobium meliloti*[a]

Strain	Doubling time (h) in:		Activity (U mg^{-1} of total protein)			
	LB-MC medium	M9-sucrose medium	6-Phosphogluconate dehydratase[b]	Aconitase[c]	Glutamate synthase[d]	Malate dehydrogenase[e]
Rm1021 (wild type)	3.2 ± 0.5	6.2 ± 0.2	102 ± 12	64 ± 10	12.9 ± 1.1	149 ± 19
SHO5 (Δ*sufT*)	5.7 ± 0.4[f]	14.9 ± 0.4[f]	10 ± 10[f]	29 ± 11[f]	6.5 ± 2.2[f]	239 ± 39[f]
SHO23 (Δ*rirA*)	ND	9.5 ± 0.8[f]	80 ± 6	106 ± 16[f]	ND	ND
SHO24 (Δ*rirA* Δ*sufT*)	ND	8.6 ± 0.8[f,g]	92 ± 28[g]	109 ± 9[f,g]	ND	ND

[a] Values are means ± SD from three or four independent measurements; ND, not determined.
[b] Expressed as nanomoles of pyruvate formed per minute. KDGP aldolase activity was 222 ± 35 in Rm1021 and 77 ± 18 in SHO5 (see Materials and Methods).
[c] Expressed as nanomoles of *cis*-aconitate formed per minute.
[d] Expressed as nanomoles of NADPH oxidized per minute.
[e] Expressed as nanomoles of NADH oxidized per minute.
[f] Significantly different from Rm1021 (*t* test, $P < 0.05$).
[g] Significantly different from SHO5 (*t* test, $P < 0.01$).

restored in HY658N by pHM102 carrying a *groESL1p-rpoH1* fusion. Therefore, the requirement for RpoH for effective symbiosis cannot be attributed solely to *sufT* upregulation, and some other key target(s) of RpoH for symbiosis remains to be identified.

Loss of SufT affects free-living growth and Fe/S cluster-dependent enzymes. The *sufT* mutant grew significantly more slowly than the wild type at 25°C in both LB-MC and M9-sucrose liquid media (Table 2). The *sufT* mutant also grew poorly on solid M9 medium containing sucrose, glucose (data not shown), or sodium succinate (Fig. 2); growth appeared similar for each carbon source (data not shown) regardless of the route of its catabolism. Sucrose and glucose are catabolized initially via the Entner-Doudoroff pathway (42), while succinate is an intermediate of the tricarboxylic acid cycle. A growth defect is plausible if SufT functions in the maintenance of Fe/S proteins involved in central metabolic pathways (e.g., 6-PGDH in the Entner-Doudoroff pathway and succinate dehydrogenase and aconitase in the tricarboxylic acid cycle), respiratory chains, or biosynthesis of amino acids and cofactors (22). In comparison with the wild type, the *sufT* mutant was more sensitive to high temperature (39°C), acidic pH (6.2), or an iron chelator which causes intracellular iron depletion (250 μM dipyridyl) when grown on LB plates (Fig. 2); all of these changes were reversed by pHM153 carrying *sufT* but not by the empty vector. Addition of $FeCl_3$ (37 μM) did not affect the differences in growth phenotypes except dipyridyl sensitivity between Rm1021 and SHO5 (data not shown). On the other hand, the survival rate of the wild type and *sufT* mutant did not significantly differ after a 30-min exposure to H_2O_2 during exponential growth (~100% at 100 μM H_2O_2 and ~10% at 250 μM H_2O_2). The *sufT* mutant and the *rpoH1* mutant sensitivities to acidic pH appeared similar (Fig. 2E). However, the *rpoH1* mutant was more sensitive to high temperature (Fig. 2B) and less sensitive to dipyridyl (Fig. 2C) than the *sufT* mutant and grew on M9 medium indistinguishably from the wild type as described previously (8) (Fig. 2F). The latter two properties imply that *sufT* is still transcribed at a basal

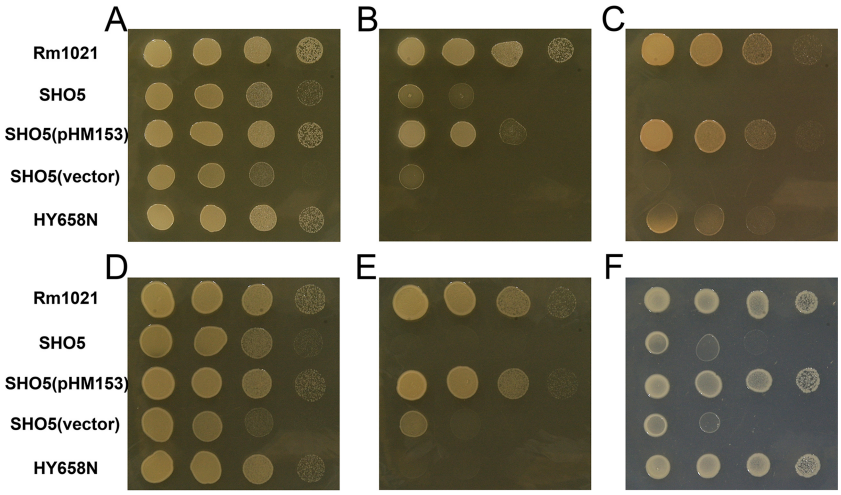

FIG 2 Growth of *Sinorhizobium meliloti* mutants on solid media. Tenfold serial dilutions (5 μl) of exponentially growing cultures (with an OD_{660} of 0.05 to 0.07) of strains Rm1021 (wild type), SHO5 (*sufT* mutant), SHO5 (harboring $sufT^+$ in the pHM153 plasmid), SHO5 (harboring the empty vector pFAJ1702), and HY658N (*rpoH1* mutant) were spotted and grown as follows: (A) LB-MC medium; 38°C for 2 days; (B) LB-MC medium; 39°C for 2 days; (C) LB medium supplemented with 2,2-dipyridyl to 250 μM; 25°C for 4 days; (D) LB medium adjusted to pH 7.0 with 35 mM 2-(*N*-morpholino)ethanesulfonic acid (MES); 25°C for 3 days; (E) LB medium adjusted to pH 6.2 with 35 mM MES; 25°C for 3 days; and (F) M9-sodium succinate medium; 25°C for 8 days. M9-sucrose and M9-glucose were also used and gave results similar to those shown in panel F (not shown in the figure). The same cultures grown with LB-MC medium were used for spots in panels A to E), and the same cultures grown with M9 medium were used for spots in panel F and on M9-sucrose and M9-glucose plates. Each of the four biological replicates gave essentially the same results in each assay.

level, supposedly from a promoter of *sufBCDS*, in the *rpoH1* mutant.

To assess an effect of the *sufT* mutation on cellular Fe/S proteins, we compared the activities of 6-PGDH, aconitase, and GltS in the wild type and *sufT* mutant. We postulated that these activities are produced by Fe/S proteins in *S. meliloti*, as in *E. coli* (22), because proteins encoded by the *E. coli* and *S. meliloti* genes are highly conserved: *edd* (6-PGDH; 59% identity; RefSeq accession numbers P0ADF6 and CAC45274 for the sequences in *E. coli* and *S. meliloti*, respectively), *acnA* (aconitase; 62%; P25516 and CAC47808), *gltB* (α subunit of GltS; 45%; P09831 and CAC47390), and *gltD* (β subunit of GltS; 38%; P09832 and CAC47389) (14). The activity of each of these enzymes was significantly lower (to a various extent) in the *sufT* mutant than in the wild type (Table 2). In contrast, the activity of malate dehydrogenase, a non-Fe/S enzyme, was increased significantly in the *sufT* mutant (Table 2). 6-PGDH and aconitase employ solvent-exposed labile [4Fe-4S] clusters as Lewis acid catalysts (43), whereas GltS has shielded [3Fe-4S] and [4Fe-4S] clusters buried in the polypeptide chains, which function in intramolecular electron transfer (44). Thus, our data suggest that SufT serves for the maintenance of various Fe/S proteins, although [2Fe-2S] cluster-containing proteins remain to be examined in this respect. An increase in malate dehydrogenase activity might be a general symptom of metabolic perturbation caused by Fe/S protein defects; indeed, this activity is markedly increased in *E. coli* mutants unable to build Fe/S clusters (27).

Loss of RirA suppresses phenotypic defects caused by the *sufT* mutation. Several rounds of culture and dilution of SHO5 cells with liquid M9-sucrose medium led to the isolation of spontaneous revertants (strains SHO8, SHO9, and SHO16) that formed visible colonies on solid M9-sucrose medium more rapidly than the original SHO5. The doubling time of these revertants (11.7 to 13.6 h) was intermediate between those of Rm1021 and SHO5 in liquid M9-sucrose medium. A deletion in *sufT* in these strains was confirmed by PCR (data not shown); therefore, we presumed that a second-site mutation suppressed the growth defect caused by the *sufT* mutation. To search for this mutation, we used whole-genome resequencing. The mutations identified are summarized in Table S6 in the supplemental material; independent deletions in *rirA* were detected in all three strains. This gene encodes an Rrf2 family transcriptional repressor in *Rhizobiaceae*, which senses the iron status possibly through the binding of the Fe/S cluster (45); accordingly, RirA serves for iron homeostasis similarly to the role of Fur proteins in many other Gram-negative and some Gram-positive bacteria (46–48). Iron overload leads to excessive generation of reactive oxygen species, and diverse bacteria tightly regulate intracellular free iron to maintain it below toxic levels (49). In *S. meliloti*, RirA represses more than 80 operons, including those involved in iron uptake under iron-replete conditions, and the *rirA* null mutation leads to iron overload that increases the sensitivity to oxidative stress (47).

To examine whether SufT and RirA are phenotypically linked, we deleted *rirA* in the *sufT* mutant background (see Fig. S2A and B in the supplemental material). In the resulting strain SHO24, 6-PGDH activity was significantly higher than that in SHO5, and aconitase activity was significantly higher than that in SHO5 and even the wild type (Table 2). SHO24 grew more rapidly than SHO5 in M9-sucrose medium (Table 2) and showed a Fix^+ phenotype (see Fig. S2C in the supplemental material) indistinguishable from that of the wild type in the plant nodulation assay. Plants inoculated with an SHO24 derivative harboring pHM186 (carrying *rirA*) exhibited a Fix^- phenotype (poor growth and small white nodules, except for a few plants that also formed a single cylindrical pink nodule), whereas plants inoculated with an SHO24 derivative harboring the empty vector exhibited a Fix^+ phenotype. Therefore, we concluded that the loss of RirA suppressed the phenotypic defects caused by the *sufT* mutation. A *rirA* single mutant (strain SHO23) is Fix^+ (47); the growth rates and Fe/S enzyme activities of the *rirA* single mutant and the *rirA sufT* double mutant were similar (Table 2; see also Fig. S2C in the supplemental material). Unlike the *sufT* mutant, the *rpoH1* mutant was not rescued by the *rirA* deletion; the *rirA rpoH1* double mutant (strain HM51) showed a Fix^- phenotype with small white nodules (data not shown). This result is consistent with the idea of some other key target(s) of RpoH for effective symbiosis, although we cannot rule out the possibility that not RirA but some other regulator acts on *in planta* iron metabolism in the *rpoH1* mutant.

DISCUSSION

Using mutational analysis, we identified *sufT* as a RpoH-dependent heat shock gene in *S. meliloti* that is indispensable for effective symbiosis. In contrast, none of the individual mutants in RpoH-dependent genes encoding major chaperones or proteases (such as ClpB, HslUV, HtpG, HtpX, and IbpA) showed appreciable symbiotic defects, as reported for the mutants lacking *groEL4* and *groESL5* (each encoding a chaperonin GroEL) (16, 50). The absence of phenotypic effects is likely due to the ability of different groups of chaperones and proteases to compensate for the loss of one of these proteins and thus maintain proteome integrity. DnaK, the major Hsp70 in bacteria, is a central organizer of the chaperone network in *E. coli* and serves for folding of the nascent polypeptides (51). We failed to disrupt *dnaK* in *S. meliloti* (data not shown), whereas this gene was not selected according to a fold change of its expression in the *rpoH1 rpoH2* mutant compared with that in the wild type in this study. The RpoH-independent operon *groESL1* is the only one sufficient for both viability and effective symbiosis among the five chaperonin-encoding operons in *S. meliloti* (50). Thus, it remains to be clarified whether an RpoH-dependent elevation, if any, of the overall chaperone/protease activities is necessary for symbiosis.

We conclude that *sufT* plays a unique role in *S. meliloti*, most probably through the maintenance of cellular Fe/S protein levels. Unlike in *S. meliloti*, its sole *E. coli* homolog *paaD* is neither regulated by σ^{32} nor linked to the *suf* locus; however, the RpoH regulon is involved in Fe/S protein metabolism in both species (4). For example, *E. coli* NfuA acts downstream of both the ISC and the SUF scaffolds to transfer Fe/S clusters to particular apoproteins under stress conditions, and its expression is regulated by σ^{32} (52, 53). Therefore, rather than indicating the specificity of the *S. meliloti* RpoH, our findings emphasize the general role of the RpoH-type sigma factors in the maintenance of protein homeostasis; these sigma factors ensure not only the proper folding and degradation of proteins but also the sufficient flux of Fe/S clusters or efficient repair of damaged Fe/S clusters in complex cellular proteins (4). The spectrum of Fe/S cluster types affected by SufT is an interesting subject for future research.

Among the components of the SUF system, the expression of only SufT and SufA is regulated by RpoH in *S. meliloti* during heat shock and acidic pH stress (18, 19). This suggests that SufT mod-

ulates the SUF system in response to heat and other stresses that impair Fe/S protein homeostasis. In *E. coli*, the loss of the two A-type carriers, SufA and IscA, is lethal under aerobic conditions (54), whereas the loss of the only known A-type carrier, SufA, still allowed for effective symbiosis in *S. meliloti*. It is not known how the loss of SufA is compensated for in *S. meliloti*; SMc02705, which contains a sequence that is partially similar to that of SufA (17% identical and 66% similar in the 51-amino acid portion; RefSeq accession numbers CAC46946 and CAC46309 for SMc02705 and SufA, respectively), is a candidate with the overlapping function. Alternatively, the A-type carrier might be dispensable for aerobic growth and symbiosis in this species.

Our study demonstrates a close relationship between the functional roles of SufT and RirA in both free-living growth and symbiosis. We consider two possible explanations for the suppression of *sufT* mutant phenotypes by the *rirA* mutation. First, the loss of the SufT function may be compensated for by increased levels of other SUF components, as the expression of *sufBCDSTA* is increased in the *S. meliloti rirA* mutant (47). It is not known whether *suf* expression is directly regulated by RirA or is affected by oxidative stress generated as a result of the *rirA* mutation. To evaluate this explanation, it is necessary to examine *sufBCDSTA* expression in the *sufT* mutant background and the effect of RirA-independent overexpression of the core SUF components and SufA on the phenotype of the *sufT* mutant. The second explanation is that a large iron pool in the *rirA* mutant increases iron flow into the SUF system, thereby compensating for the lack of SufT. We showed that the depletion of the intracellular iron pool with dipyridyl rendered SufT indispensable for the growth in rich medium. Therefore, we propose that SufT serves to balance the intrinsic iron limitation exerted by RirA so that SufT function becomes crucial under conditions adverse to iron homeostasis. In this case, the effect of SufT on iron acquisition by the SUF system would be indirect, because its homologs, such as human CIA2B, appear to act at a late step of the Fe/S protein biogenesis pathway, i.e., transfer of preassembled Fe/S clusters to target apoproteins (39). Yet, this explanation does not appear consistent with the findings in *E. coli* and some other bacteria, in which, despite the lack of a SufT ortholog, the SUF system appears to build and transfer Fe/S clusters in a more oxidant-resistant way than the housekeeping ISC system and is induced and replaces ISC as the main pathway under adverse conditions (24, 55–58). It would be important to examine whether the function of each SUF component varies between *S. meliloti* and *E. coli*. Interestingly, SufD is much less conserved (29% identity; RefSeq accession numbers CAC46312 and P77689 for the sequences in *S. meliloti* and *E. coli*, respectively) than SufB (59%; CAC46314 and P77522) and SufC (58%; CAC46313 and P77499) between these organisms. Since SufD was shown to contribute to iron acquisition by the scaffold in *E. coli* (59), the difference in the SufD structure might affect the entrance of iron into the SUF system so that Fe/S clusters could be assembled efficiently without SufT in *E. coli* but not in *S. meliloti*.

From a viewpoint of the relationship between RpoH and iron metabolism, it is noteworthy that expression of the rhizobactin synthesis genes *rhbABCDEF* and the rhizobactin transporter gene *rhtA* is increased, while expression of the transcriptional activator gene *rhrA* is decreased, in the *rpoH1* mutant compared with that in the wild type under a neutral pH and no heat shock condition (18). Rhizobactin is an *S. meliloti*-produced siderophore, which binds to ferric iron for iron acquisition, and its synthesis and transport genes are transcribed with the action of RhrA, whose expression is repressed by RirA in turn (47). Expression of the rhizobactin-related genes might be affected by perturbations in iron homeostasis as a result of the failure to increase *sufT* expression in the *rpoH1* mutant. Examination of an effect of the loss of RpoH1 or SufT on the Fe/S cluster-binding status of RirA will possibly provide a clue to the puzzling pattern of rhizobactin-related gene expression.

Why is the *sufT* mutant deficient in symbiosis? First, a larger variety of *S. meliloti* Fe/S proteins participate in symbiosis than in free-living growth in rich media. For optimal nodulation and infection, *S. meliloti* needs to synthesize branched-chain amino acids (isoleucine, valine, and leucine) (60), and their biosynthesis involves Fe/S proteins such as IlvD and LeuC (22). An active nitrogenase complex contains a [4Fe-4S] cluster and more complex clusters such as the P cluster [8Fe-7S] and the iron-molybdenum cofactor [7Fe-9S-1C-1Mo-homocitrate] (61). Second, interactions with the plant may adversely affect iron homeostasis in *S. meliloti*. The absence of deleterious iron overload in the *rirA* mutant during symbiosis suggests that *S. meliloti* acquires only a limited amount of iron from the host (47). In addition, *S. meliloti* is exposed to reactive oxygen and nitrogen species, which are produced by the host as modulators of nodule development and by *S. meliloti* owing to the high respiration rates necessary for nitrogen fixation (62). *Sinorhizobium meliloti* needs to compensate for the oxidative loss of Fe/S clusters caused by those reactive species (43). Therefore, chronic oxidative stress under iron limitation might necessitate the function of SufT, although the *sufT* mutation did not affect survival after short-term H_2O_2 treatment in our experiments. We conclude that *S. meliloti* needs SufT to produce sufficient amounts of Fe/S proteins during symbiosis. A decrease in symbiotic performance possibly linked to Fe/S cluster metabolism has also been reported for an *S. meliloti* mutant lacking the monothiol glutaredoxin SmGRX2, which is attenuated in nitrogen fixation capacity (63). Monothiol glutaredoxins have been suggested to serve for delivery of [2Fe-2S] clusters in some bacteria and eukaryotes (23).

In addition to Fe/S protein biogenesis, the RpoH regulon also affects redox control using glutathione through its members *gshB1* (encoding glutathione synthetase) and *grxC* (encoding the dithiol glutaredoxin SmGRX1) (18, 19). The *gshB1* mutant displays early senescence of bacteroids (64). SmGRX1 contributes to protein deglutathionylation, and its null mutant is defective in nodule development and bacteroid differentiation (63). The expression of *rpoH1* and several RpoH-regulated genes, including *sufT* and *grxC*, is increased by NCR peptides (65, 66), suggesting that these genes are incorporated into a complex regulatory network that allows bacteria to adapt to the host cell environment. Thus, the RpoH function serves for the robustness of symbiosis when *S. meliloti* is exposed to Fe/S cluster-damaging oxidative stress.

ACKNOWLEDGMENTS

We thank Yoshiyuki Ohtsubo for advice on the use of ShortReadManager, Kaori Kakizaki for advice on the use of MiSeq, and Akiko Kudo and Akemi Saito for technical assistance in strain construction.

This work was supported by Grants-in-Aid for Scientific Research (grants 22380048 and 16K07654) to H.M. from the Japan Society for the Promotion of Science.

FUNDING INFORMATION

This work, including the efforts of Hisayuki Mitsui, was funded by Japan Society for the Promotion of Science (JSPS) (16K07654 and 22380048).

REFERENCES

1. **Gibson KE, Kobayashi H, Walker GC.** 2008. Molecular determinants of a symbiotic chronic infection. Annu Rev Genet **42:**413–441. http://dx.doi.org/10.1146/annurev.genet.42.110807.091427.
2. **Oldroyd GED, Murray JD, Poole PS, Downie A.** 2011. The rules of engagement in the legume-rhizobial symbiosis. Annu Rev Genet **45:**119–144. http://dx.doi.org/10.1146/annurev-genet-110410-132549.
3. **Feklístov A, Sharon BD, Darst SA, Gross CA.** 2014. Bacterial sigma factors: a historical, structural, and genomic perspective. Annu Rev Microbiol **68:**357–376. http://dx.doi.org/10.1146/annurev-micro-092412-155737.
4. **Guisbert E, Yura T, Rhodius VA, Gross CA.** 2008. Convergence of molecular, modeling, and systems approaches for an understanding of the *Escherichia coli* heat shock response. Microbiol Mol Biol Rev **72:**545–554. http://dx.doi.org/10.1128/MMBR.00007-08.
5. **Kim YE, Hipp MS, Bracher A, Hayer-Hartl M, Hartl FU.** 2013. Molecular chaperone functions in protein folding and proteostasis. Annu Rev Biochem **82:**323–355. http://dx.doi.org/10.1146/annurev-biochem-060208-092442.
6. **Nakahigashi K, Yanagi H, Yura T.** 1995. Isolation and sequence analysis of *rpoH* genes encoding σ^{32} homologs from Gram negative bacteria: conserved mRNA and protein segments for heat shock regulation. Nucleic Acids Res **23:**4383–4390.
7. **Nakahigashi K, Ron EZ, Yanagi H, Yura T.** 1999. Differential and independent roles of a σ^{32} homolog (RpoH) and an HrcA repressor in the heat shock response of *Agrobacterium tumefaciens*. J Bacteriol **181:**7509–7515.
8. **Ono Y, Mitsui H, Sato T, Minamisawa K.** 2001. Two RpoH homologs responsible for the expression of heat shock protein genes in *Sinorhizobium meliloti*. Mol Gen Genet **264:**902–912. http://dx.doi.org/10.1007/s004380000380.
9. **Slamti L, Livny J, Waldor MK.** 2007. Global gene expression and phenotypic analysis of a *Vibrio cholerae rpoH* deletion mutant. J Bacteriol **189:**351–362. http://dx.doi.org/10.1128/JB.01297-06.
10. **Ueki T, Lovley DR.** 2007. Heat-shock sigma factor RpoH from *Geobacter sulfurreducens*. Microbiology **153:**838–846. http://dx.doi.org/10.1099/mic.0.2006/000638-0.
11. **Dufour YS, Imam S, Koo B-M, Green HA, Donohue TJ.** 2012. Convergence of the transcriptional responses to heat shock and singlet oxygen stresses. PLoS Genet **8:**e1002929. http://dx.doi.org/10.1371/journal.pgen.1002929.
12. **Martínez-Salazar JM, Sandoval-Calderón M, Guo X, Castillo-Ramírez S, Reyes A, Loza MG, Rivera J, Alvarado-Affantranger X, Sánchez F, González V, Dávila G, Ramírez-Romero MA.** 2009. The *Rhizobium etli* RpoH1 and RpoH2 sigma factors are involved in different stress responses. Microbiology **155:**386–397. http://dx.doi.org/10.1099/mic.0.021428-0.
13. **Oke V, Rushing BG, Fisher EJ, Moghadam-Tabrizi M, Long SR.** 2001. Identification of the heat-shock sigma factor RpoH and a second RpoH-like protein in *Sinorhizobium meliloti*. Microbiology **147:**2399–2408. http://dx.doi.org/10.1099/00221287-147-9-2399.
14. **Galibert F, Finan TM, Long SR, Puhler A, Abola P, Ampe F, Barloy-Hubler F, Barnett MJ, Becker A, Boistard P, Bothe G, Boutry M, Bowser L, Buhrmester J, Cadieu E, Capela D, Chain P, Cowie A, Davis RW, Dréano S, Federspiel NA, Fisher RF, Gloux S, Godrie T, Goffeau A, Golding B, Gouzy J, Gurjal M, Hernandez-Lucas I, Hong A, Huizar L, Hyman RW, Jones T, Kahn D, Kahn ML, Kalman S, Keating DH, Kiss E, Komp C, Lelaure V, Masuy D, Palm C, Peck MC, Pohl TM, Portetelle D, Purnelle B, Ramsperger U, Surzycki R, Thébault P, Vandenbol M, Vorhölter F-J, Weidner S, Wells DH, Wong K, Yeh K-C, Batut J.** 2001. The composite genome of the legume symbiont *Sinorhizobium meliloti*. Science **293:**668–672. http://dx.doi.org/10.1126/science.1060966.
15. **Narberhaus F, Krummenacher P, Fischer H-M, Hennecke H.** 1997. Three disparately regulated genes for σ^{32}-like transcription factors in *Bradyrhizobium japonicum*. Mol Microbiol **24:**93–104. http://dx.doi.org/10.1046/j.1365-2958.1997.3141685.x.
16. **Mitsui H, Sato T, Sato Y, Ito N, Minamisawa K.** 2004. *Sinorhizobium meliloti* RpoH1 is required for effective nitrogen-fixing symbiosis with alfalfa. Mol Genet Genomics **271:**416–425. http://dx.doi.org/10.1007/s00438-004-0992-x.
17. **Bittner AN, Oke V.** 2006. Multiple *groESL* operons are not key targets of RpoH1 and RpoH2 in *Sinorhizobium meliloti*. J Bacteriol **188:**3507–3515. http://dx.doi.org/10.1128/JB.188.10.3507-3515.2006.
18. **de Lucena DK, Pühler A, Weidner S.** 2010. The role of sigma factor RpoH1 in the pH stress response of *Sinorhizobium meliloti*. BMC Microbiol **10:**265. http://dx.doi.org/10.1186/1471-2180-10-265.
19. **Barnett MJ, Bittner AN, Toman CJ, Oke V, Long SR.** 2012. Dual RpoH sigma factors and transcriptional plasticity in a symbiotic bacterium. J Bacteriol **194:**4983–4994. http://dx.doi.org/10.1128/JB.00449-12.
20. **Beinert H, Holm RH, Münck E.** 1997. Iron-sulfur clusters: nature's modular, multipurpose structures. Science **277:**653–659. http://dx.doi.org/10.1126/science.277.5326.653.
21. **Lill R.** 2009. Function and biogenesis of iron-sulphur proteins. Nature **460:**831–838. http://dx.doi.org/10.1038/nature08301.
22. **Py B, Barras F.** 2010. Building Fe-S proteins: bacterial strategies. Nat Rev Microbiol **8:**436–446. http://dx.doi.org/10.1038/nrmicro2356.
23. **Roche B, Aussel L, Ezraty B, Mandin P, Py B, Barras F.** 2013. Iron/sulfur proteins biogenesis in prokaryotes: formation, regulation and diversity. Biochim Biophys Acta **1827:**455–469. http://dx.doi.org/10.1016/j.bbabio.2012.12.010.
24. **Boyd ES, Thomas KM, Dai Y, Boyd JM, Outten FW.** 2014. Interplay between oxygen and Fe-S cluster biogenesis: insights from the Suf pathway. Biochemistry **53:**5834–5847. http://dx.doi.org/10.1021/bi500488r.
25. **Outten FW.** 2015. Recent advances in the Suf Fe-S cluster biogenesis pathway: beyond the proteobacteria. Biochim Biophys Acta **1853:**1464–1469. http://dx.doi.org/10.1016/j.bbamcr.2014.11.001.
26. **Tan G, Lu J, Bitoun JP, Huang H, Ding H.** 2009. IscA/SufA paralogues are required for the [4Fe-4S] cluster assembly in enzymes of multiple physiological pathways in *Escherichia coli* under aerobic growth conditions. Biochem J **420:**463–472. http://dx.doi.org/10.1042/BJ20090206.
27. **Tanaka N, Kanazawa M, Tonosaki K, Yokoyama N, Kuzuyama T, Takahashi Y.** 2016. Novel features of the ISC machinery revealed by characterization of *Escherichia coli* mutants that survive without iron-sulfur clusters. Mol Microbiol **99:**835–848. http://dx.doi.org/10.1111/mmi.13271.
28. **Miller JH.** 1992. A short course in bacterial genetics: a laboratory manual and handbook for *Escherichia coli* and related bacteria. CSHL Press, Cold Spring Harbor, NY.
29. **Finan TM, Hartwieg E, LeMieux K, Bergman K, Walker GC, Signer ER.** 1984. General transduction in *Rhizobium meliloti*. J Bacteriol **159:**120–124.
30. **Somasegaran P, Hoben HJ.** 1994. Handbook for rhizobia: methods in legume-rhizobium technology. Springer-Verlag, New York, NY.
31. **Finan TM, Kunkel B, De Vos GF, Signer ER.** 1986. Second symbiotic megaplasmid in *Rhizobium meliloti* carrying exopolysaccharide and thiamine synthesis genes. J Bacteriol **167:**66–72.
32. **Fraenkel DG, Horecker BL.** 1964. Pathways of D-glucose metabolism in *Salmonella typhimurium*. J Biol Chem **239:**2765–2771.
33. **Henson CP, Cleland WW.** 1967. Purification and kinetic studies of beef liver cytoplasmic aconitase. J Biol Chem **242:**3833–3838.
34. **Miller RE, Stadtman ER.** 1972. Glutamate synthase from *Escherichia coli*. An iron-sulfide flavoprotein. J Biol Chem **247:**7407–7419.
35. **Kitto GB.** 1969. Intra- and extramitochondrial malate dehydrogenase from chicken and tuna heart. Methods Enzymol **13:**106–116. http://dx.doi.org/10.1016/0076-6879(69)13023-2.
36. **Ohtsubo Y, Maruyama F, Mitsui H, Nagata Y, Tsuda M.** 2012. Complete genome sequence of *Acidovorax* sp. strain KKS102, a polychlorinated-biphenyl degrader. J Bacteriol **194:**6970–6971. http://dx.doi.org/10.1128/JB.01848-12.
37. **Schlüter J-P, Reinkensmeier J, Barnett MJ, Lang C, Krol E, Giegerich R, Long SR, Becker A.** 2013. Global mapping of transcription start sites and promoter motifs in the symbiotic α-proteobacterium *Sinorhizobium meliloti* 1021. BMC Genomics **14:**156. http://dx.doi.org/10.1186/1471-2164-14-156.
38. **Teufel R, Friedrich T, Fuchs G.** 2012. An oxygenase that forms and deoxygenates toxic epoxide. Nature **483:**359–362. http://dx.doi.org/10.1038/nature10862.
39. **Stehling O, Mascarenhas J, Vashisht AA, Sheftel AD, Niggemeyer B, Rösser R, Pierik AJ, Wohlschlegel JA, Lill R.** 2013. Human CIA2A-FAM96A and CIA2B-FAM96B integrate iron homeostasis and matura-

tion of different subsets of cytosolic-nuclear iron-sulfur proteins. Cell Metab **18:**187–198. http://dx.doi.org/10.1016/j.cmet.2013.06.015.
40. **Lezhneva L, Aman K, Meuer J.** 2004. The universally conserved HCF101 protein is involved in assembly of [4Fe-4S]-cluster-containing complexes in *Arabidopsis thaliana* chloroplasts. Plant J **37:**174–185. http://dx.doi.org/10.1046/j.1365-313X.2003.01952.x.
41. **Huet G, Daffé M, Saves I.** 2005. Identification of the *Mycobacterium tuberculosis* SUF machinery as the exclusive mycobacterial system of [Fe-S] cluster assembly: evidence for its implication in the pathogen's survival. J Bacteriol **187:**6137–6146. http://dx.doi.org/10.1128/JB.187.17.6137-6146.2005.
42. **Fuhrer T, Fischer E, Sauer U.** 2005. Experimental identification and quantification of glucose metabolism in seven bacterial species. J Bacteriol **187:**1581–1590. http://dx.doi.org/10.1128/JB.187.5.1581-1590.2005.
43. **Imlay JA.** 2008. Cellular defenses against superoxide and hydrogen peroxide. Annu Rev Biochem **77:**755–776. http://dx.doi.org/10.1146/annurev.biochem.77.061606.161055.
44. **Vanoni MA, Curti B.** 1999. Glutamate synthase: a complex iron-sulfur flavoprotein. Cell Mol Life Sci **55:**617–638. http://dx.doi.org/10.1007/s000180050319.
45. **Mettert EL, Kiley PJ.** 2015. Fe-S proteins that regulate gene expression. Biochim Biophys Acta **1853:**1284–1293. http://dx.doi.org/10.1016/j.bbamcr.2014.11.018.
46. **Todd JD, Wexler M, Sawers G, Yeoman KH, Poole PS, Johnston AWB.** 2002. RirA, an iron-responsive regulator in the symbiotic bacterium *Rhizobium leguminosarum*. Microbiology **148:**4059–4071. http://dx.doi.org/10.1099/00221287-148-12-4059.
47. **Chao T-C, Buhrmester J, Hansmeier N, Pühler A, Weidner S.** 2005. Role of regulatory gene *rirA* in the transcriptional response of *Sinorhizobium meliloti* to iron limitation. Appl Environ Microbiol **71:**5969–5982. http://dx.doi.org/10.1128/AEM.71.10.5969-5982.2005.
48. **Viguier C, Cuív PO, Clarke P, O'Connell M.** 2005. RirA is the iron response regulator of the rhizobactin 1021 biosynthesis and transport genes in *Sinorhizobium meliloti* 2011. FEMS Microbiol Lett **246:**235–242. http://dx.doi.org/10.1016/j.femsle.2005.04.012.
49. **Touati D.** 2000. Iron and oxidative stress in bacteria. Arch Biochem Biophys **373:**1–6. http://dx.doi.org/10.1006/abbi.1999.1518.
50. **Bittner AN, Foltz A, Oke V.** 2007. Only one of five *groEL* genes is required for viability and successful symbiosis in *Sinorhizobium meliloti*. J Bacteriol **189:**1884–1889. http://dx.doi.org/10.1128/JB.01542-06.
51. **Calloni G, Chen T, Schermann SM, Chang H-C, Genevaux P, Agostini F, Tartaglia GG, Hayer-Hartl M, Hartl FU.** 2012. DnaK functions as a central hub in the *E. coli* chaperone network. Cell Rep **1:**251–264. http://dx.doi.org/10.1016/j.celrep.2011.12.007.
52. **Nonaka G, Blankschien M, Herman C, Gross CA, Rhodius VA.** 2006. Regulon and promoter analysis of the *E. coli* heat-shock factor, σ^{32}, reveals a multifaceted cellular response to heat stress. Genes Dev **20:**1776–1789. http://dx.doi.org/10.1101/gad.1428206.
53. **Py B, Gerez C, Angelini S, Planel R, Vinella D, Loiseau L, Talla E, Brochier-Armanet C, Serres RG, Latour J-M, Ollagnier-de Choudens S, Fontecave M, Barras F.** 2012. Molecular organization, biochemical function, cellular role and evolution of NfuA, an atypical Fe-S carrier. Mol Microbiol **86:**155–171. http://dx.doi.org/10.1111/j.1365-2958.2012.08181.x.
54. **Vinella D, Brochier-Armanet C, Loiseau L, Talla E, Barras F.** 2009. Iron-sulfur (Fe/S) protein biogenesis: phylogenomic and genetic studies of A-type carriers. PLoS Genet **5:**e1000497. http://dx.doi.org/10.1371/journal.pgen.1000497.
55. **Nachin L, Hassouni ME, Loiseau L, Expert D, Barras F.** 2001. SoxR-dependent response to oxidative stress and virulence of *Erwinia chrysanthemi*: the key role of SufC, and orphan ABC ATPase. Mol Microbiol **39:**960–972. http://dx.doi.org/10.1046/j.1365-2958.2001.02288.x.
56. **Outten FW, Djaman O, Storz G.** 2004. A *suf* operon requirement for Fe-S cluster assembly during iron starvation in *Escherichia coli*. Mol Microbiol **52:**861–872. http://dx.doi.org/10.1111/j.1365-2958.2004.04025.x.
57. **Tokumoto U, Kitamura S, Fukuyama K, Takahashi Y.** 2004. Interchangeability and distinct properties of bacterial Fe-S cluster assembly systems: functional replacement of the *isc* and *suf* operons in *Escherichia coli* with the *nifSU*-like operon from *Helicobacter pylori*. J Biochem **136:**199–209. http://dx.doi.org/10.1093/jb/mvh104.
58. **Jang S, Imlay JA.** 2010. Hydrogen peroxide inactivates the *Escherichia coli* Isc iron-sulphur assembly system, and OxyR induces the Suf system to compensate. Mol Microbiol **78:**1448–1467. http://dx.doi.org/10.1111/j.1365-2958.2010.07418.x.
59. **Saini A, Mapolelo DT, Chahal HK, Johnson MK, Outten FW.** 2010. SufD and SufC ATPase activity are required for iron acquisition during in vivo Fe-S cluster formation on SufB. Biochemistry **49:**9402–9412. http://dx.doi.org/10.1021/bi1011546.
60. **de las Nieves Peltze M, Roques N, Poinsot V, Aguilar OM, Batut J, Capela D.** 2008. Auxotrophy accounts for nodulation defect of most *Sinorhizobium meliloti* mutants in the branched-chain amino acid biosynthesis pathway. Mol Plant Microbe Interact **21:**1232–1241. http://dx.doi.org/10.1094/MPMI-21-9-1232.
61. **Peters JW, Broderick JB.** 2012. Emerging paradigms for complex iron-sulfur cofactor assembly and insertion. Annu Rev Biochem **81:**429–450. http://dx.doi.org/10.1146/annurev-biochem-052610-094911.
62. **Ribeiro CW, Alloing G, Mandon K, Frendo P.** 2015. Redox regulation of differentiation in symbiotic nitrogen fixation. Biochim Biophys Acta **1850:**1469–1478. http://dx.doi.org/10.1016/j.bbagen.2014.11.018.
63. **Benyamina SM, Baldacci-Cresp F, Couturier J, Chibani K, Hopkins J, Bekki A, de Lajudie P, Rouhier N, Jacquot J-P, Alloing G, Puppo A, Frendo P.** 2013. Two *Sinorhizobium meliloti* glutaredoxins regulate iron metabolism and symbiotic bacteroid differentiation. Environ Microbiol **15:**795–810. http://dx.doi.org/10.1111/j.1462-2920.2012.02835.x.
64. **Harrison J, Jamet A, Muglia CI, Van de Sype G, Aguilar OM, Puppo A, Frendo P.** 2005. Glutathione plays a fundamental role in growth and symbiotic capacity of *Sinorhizobium meliloti*. J Bacteriol **187:**168–174. http://dx.doi.org/10.1128/JB.187.1.168-174.2005.
65. **Tiricz H, Szűcs A, Farkas A, Pap B, Lima RM, Maróti G, Kondorosi E, Kereszt A.** 2013. Antimicrobial nodule-specific cysteine-rich peptides induce membrane depolarization-associated changes in the transcriptome of *Sinorhizobium meliloti*. Appl Environ Microbiol **79:**6737–6746. http://dx.doi.org/10.1128/AEM.01791-13.
66. **Penterman J, Abo RP, De Nisco NJ, Arnold MFF, Longhi R, Zanda M, Walker GC.** 2014. Host plant peptides elicit a transcriptional response to control the *Sinorhizobium meliloti* cell cycle during symbiosis. Proc Natl Acad Sci U S A **111:**3561–3566. http://dx.doi.org/10.1073/pnas.1400450111.
67. **Almeida MS, Herrmann T, Peti W, Wilson IA, Wüthrich K.** 2005. NMR structure of the conserved hypothetical protein TM0487 from *Thermotoga maritima*: implications for 216 homologous DUF59 proteins. Protein Sci **14:**2880–2886. http://dx.doi.org/10.1110/ps.051755805.
68. **Weerapana E, Wang C, Simon GM, Richter F, Khare S, Dillon MBD, Bachovchin D, Mowen K, Baker D, Cravatt BF.** 2010. Quantitative reactivity profiling predicts functional cysteines in proteomes. Nature **468:**790–795. http://dx.doi.org/10.1038/nature09472.
69. **Meade HM, Long SR, Ruvkun GB, Brown SE, Ausubel FM.** 1982. Physical and genetic characterization of symbiotic and auxotrophic mutants of *Rhizobium meliloti* induced by transposon Tn5 mutagenesis. J Bacteriol **149:**114–122.
70. **Becker A, Schmidt M, Jäger W, Pühler A.** 1995. New gentamicin-resistance and *lacZ* promoter-probe cassettes suitable for insertion mutagenesis and generation of transcriptional fusions. Gene **162:**37–39. http://dx.doi.org/10.1016/0378-1119(95)00313-U.
71. **Prentki P, Krisch HM.** 1984. In vitro insertional mutagenesis with a selectable DNA fragment. Gene **29:**303–313. http://dx.doi.org/10.1016/0378-1119(84)90059-3.
72. **Schäfer A, Tauch A, Jäger W, Kalinowski J, Thierbach G, Pühler A.** 1994. Small mobilizable multi-purpose cloning vectors derived from the *Escherichia coli* plasmids pK18 and pK19: selection of defined deletions in the chromosome of *Corynebacterium glutamicum*. Gene **145:**69–73. http://dx.doi.org/10.1016/0378-1119(94)90324-7.
73. **Maseda H, Hashida Y, Konaka R, Shirai A, Kourai H.** 2009. Mutational upregulation of a resistance-nodulation-cell division-type multidrug efflux pump, SdeAB, upon exposure to a biocide, cetylpyridinium chloride, and antibiotic resistance in *Serratia marcescens*. Antimicrob Agents Chemother **53:**5230–5235. http://dx.doi.org/10.1128/AAC.00631-09.
74. **Dombrecht B, Vanderleyden J, Michiels J.** 2001. Stable RK2-derived cloning vectors for the analysis of gene expression and gene function in Gram-negative bacteria. Mol Plant Microbe Interact **14:**426–430. http://dx.doi.org/10.1094/MPMI.2001.14.3.426.
75. **Cheng H-P, Walker GC.** 1998. Succinoglycan is required for initiation and elongation of infection threads during nodulation of alfalfa by *Rhizobium meliloti*. J Bacteriol **180:**5183–5191.